Analytical Methods

Accepted Manuscript

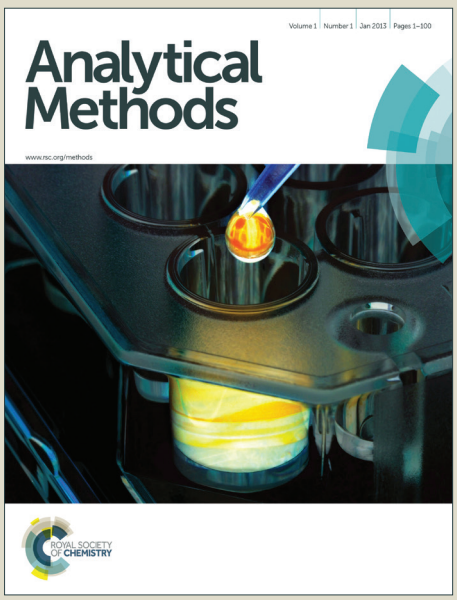

ROYAL SOCIETY OF CHEMISTRY

www.rsc.org/methods

Graphical abstract

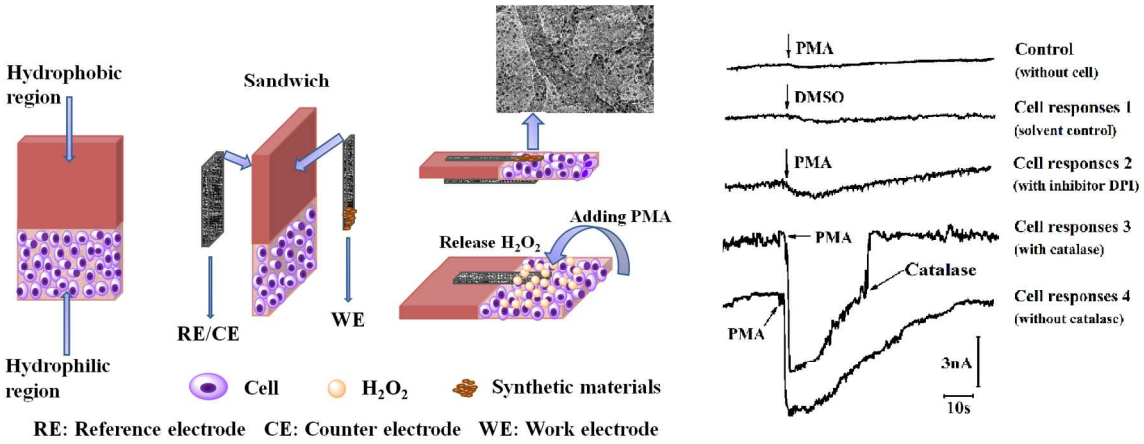

The CNT/graphene/MnO_2 nanocomposite decorated electrodes/paper sandwich devices real-time sensing hydrogen peroxide released from cells growing in paper 3 dimensional matrix, offering new insights on designing disposable miniaturized biosensors for cell biology investigations.

Cite this: DOI: 10.1039/c0xx00000x

www.rsc.org/xxxxxx

ARTICLE TYPE

Electrodes/paper sandwich devices for in situ sensing of hydrogen peroxide secretion from cells growing in gels-in-paper 3 dimensional matrix

ZhuanZhuan Shi,[a,b,c] XiaoShuai Wu,[a,b,c] LiXia Gao,[a,b,c] YunLi Tian[a,b,c] and Ling Yu*[a,b,c]

Received (in XXX, XXX) XthXXXXXXXXX 20XX, Accepted Xth XXXXXXXXX 20XX
DOI: 10.1039/b000000x

In the present study, a carbon paper electrode (CPE)/cells-in-paper/CPE sandwich device was developed for in situ detection small molecular produced from cells growing in paper 3 dimensional matrix. To demonstrate the real-time assay capability of the electrodes/cells-in-paper sandwich device, carbon nanotube/graphene/MnO_2 nanocomposite was synthesized to functionalize the working electrode. The Scanning electron microscopy, transmission electron microscope and X-ray photoelectron spectroscopy characterization prove that MnO_2 nanoparitcles uniformly distributed on nanotube sidewalls and graphene sheets. The carbon nanotube/graphene/MnO_2 nanocomposite functionalized electrode/cells-in-paper sandwich device showed specific response against hydrogen peroxide. The fully assembled device displays a linear range up to 25 mM with a sensitivity of 6.25 $\mu AmM^{-1}cm^{-2}$, and a detection limit of 6.7 μM hydrogen peroxide. In addition, *in situ* detection of hydrogen peroxide production from cells growing in matrigel impregnated paper was successfully demonstrated on the electrodes/cells-in-paper sandwich device, highlighting the potential application of this low-cost paper analytical devices for cell biology studies.

1. Introduction

As a three-dimensional (3D) cellulose fiber network, paper attracts tremendous attentions for fabrication of bio-sensing devices due to its exhibited advantages.[1-3] Its ease of use and storage empower it as a promising economical biocompatible material for fabrication of disposable biosensors. Moreover, the porous cellulose fiber networks of paper acts as capillaries, wicking aqueous solutions without the need for active pumping. Therefore, researchers in the bio-analytical community have paid significant efforts to construct highly sensitive, operationally simple and low-cost paper-based analytical devices (PADs).[4, 5] Different detection scheme have been demonstrated on PADs, such as colorimetric, chemilluminances, electrochemistry and surface-enhanced Raman scattering etc.[3, 6-10] In most of the case, PADs sensors are developed for protein analyse. For instance, in Zang's work, sandwich immunoassay reaction scheme for cancer markers, α-fetoprotein and carcinoma antigen, has been demonstrated on a 3D microfluidic paper-based device.[11] Nie *et al* has highlighted the PAD's low-cost advantages in blood glucose sensing.[6]

As a basic functional unit of life, cell based biochemical analysis provides crucial information for biological and medical issues. There is a need to construct a stable, simple and sensitive analytic device for monitoring of cell metabolism status. However, currently, cell-based assays strongly rely on 2 dimensional (2D) cell culture systems that lack the capability to recapitulate the structure, function and physiology of *in vivo* cell growth. Microfabrication can create architecturally complex scaffolds for 3D cell cultures.[12-14] However, these approaches require instruments that are not commonly available in biology laboratories. One significant breakthrough is the development of a "cells-in-gels-in-paper" 3D cell culture system by layers of paper impregnated with cell suspensions in hydrogel for analyzing molecular and genetic responses of cells.[15-17] Herein, it is of highly interests to develop a PAD incorporated with a 3D cell culture platform to *in situ* measure the activity of cells that are growing in an environment mimics *in vivo* conditions. To demonstrate the biological significant of the cell-PAD sensor, we detected the hydrogen peroxide (H_2O_2) production from human tumor cells since H_2O_2 plays important roles in many cellular signaling pathways impacting on cell proliferation, activation migration *etc*.[18] Due to its biological significance, efforts have been paid to design and construct biosensors to examine hydrogen peroxide.[19] Enzymes, such as HRP and catalase, have been immobilized on electrode for H_2O_2 sensing.[20, 21] Progressively, non-enzyme sensing materials became an economical alternative.[22-25] For instance, prussian blue, a kind of artificial peroxidase, was composited with carbon nanotubes (CNTs),[26] mesoporous carbons[27] or layered graphene[25] to achieve H_2O_2 detection. Manganese dioxide (MnO_2) is another attractive inorganic oxide material towards H_2O_2 sensing because of the excellent catalytic ability of MnO_2 nanoparticles.[28] Zhang *et al* reported a direct electro catalytic oxidation of H_2O_2 based on nafion and microspheres MnO_2 modified glass carbon electrode.[29]

While, a MnO_2/graphene oxide nanocompoiste functionalized glass carbon electrode realized detection of H_2O_2 in alkaline medium.[30] Most recently, growing of MnO_2 on carbon nanotube derived graphene for hydrogen peroxide detection has been reported.[31, 32] However, the peeling of graphene layer from carbon nanotube should be conducted in an extraordinary hush condition. From the SEM characterization, morphology of the synthesized material was similar to carbon nanotubes and no tenuous networks of clustered nanoparticles can be observed. Because of the excellent electrical conductivity and high specific surface-area-to-volume ratio, CNT/graphene aerogel have been applied for supercapacitor and biosensing.[33-35] Thus, we anticipated to grow MnO_2 nanoparticles on CNT/graphene aerogel to achieve high electrochemical activity for the detection of cell secreted H_2O_2.

Although plenty of electrochemical sensors for hydrogen peroxide were reported, the majority of them utilized glass carbon electrode and indium tin oxide (ITO) glass to measure H_2O_2 in a standard three-electrode systems.[25, 27, 29, 30, 36-38] Thus, it is impractical for them as a candidate for economical disposable device application. Moreover, few of them achieved *in situ*, particularly selective and quantitative, detection of H_2O_2 secreted by living cells.[21, 25, 36] Due to the significance of cell biology to medical science, it is highly anticipated a simplified, disposable device to fulfilled the functions of traditional three-electrodes electrochemical analysing system. The enthusiasm will be strengthen if the device could assay H_2O_2 in a 3D cell growth model, while providing reliable diagnosis of pathological conditions. In the present study, we fabricated an electrode/cells-in-paper sandwich device to realize the *in situ* sensing of H_2O_2 production from cells growing in paper 3-dimensional matrix. To achieve this aim, carbon nanotube/graphene/MnO_2composite functionalized carbon paper electrode sandwiched with wax-printed paper which functional as a 3D matrix to sustain cell growth to *in situ* monitor extracellular hydrogen peroxide produced by human cells. Scanning electron microscopy (SEM), transmission electron microscope (TEM) and X-ray photoelectron spectroscopy (XPS) characterized the synthesized carbon nanotube/graphene/MnO_2 aerogel. The fully assembled nanocomposite functionalized electrodes/paper sandwich device *in situ* sensed the response of larynx carcinoma cells upon the stimulation of phorbol 12-myristate-13-acetate (PMA). The experiment results confirmed that the fully assembled electrode/cells-in-paper sandwich device was indeed *in situ* monitoring H_2O_2 generated by human cells, highlighting the potential application of electrodes/paper devices in cell biology study and drug screening.

2. Materials and methods

2.1 Materials

Carbon paper TGP-H-060 (thickness: 0.17 cm) was purchased from Toray Ind. (Japan). Graphite, WMCNT, ascorbic acid, 30% hydrogen peroxide, potassium hexacyanoferrate(III) ($K_3[Fe(CN)_6]$), nafion phosphate buffered saline(PBS) and potassium permanganate ($KMnO_4$) were all purchased from Aladdin, China. Human larynx carcinoma cell line HEp2 was general gift from Dr. Yuan Li, Chongqing Medical University. The cells are maintained in RPMI1640 medium (Gibco) with 10% fetal bovine serum (Gibco), 100 μg mL^{-1} penicillin and 100 μg mL^{-1} streptomycin. Phorbol 12-myristate-13-acetate (PMA), diphenyleneiodonium (DPI), catalase, dopamine, and uric acid were purchased from Sigma Aldrich. The glass filter paper (CB08) was purchased from Shanghai Kinbio Tech (China). All other chemical used in this study were analytical grade. The deionized (DI) water used in all experiments is produced by PURELAB flex system, ELGA Corporation.

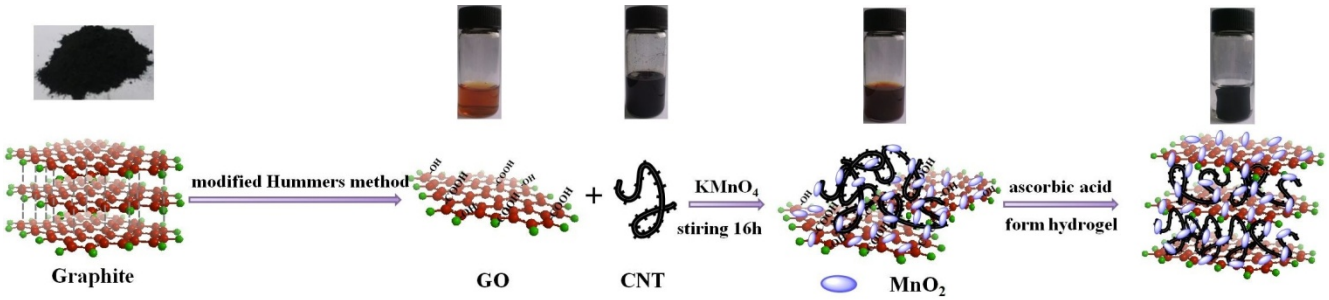

Scheme 1. Schematic illustration of the fabrication of CNT/graphene/MnO_2 hydrogel. GO: graphene oxide, CNT: carbon nanotube, MnO_2: manganese dioxide

2.2 Synthesis of CNT/graphene/MnO_2 aerogel

The graphene oxide used in this work was prepared from graphite by using a modified Hummers method.[39] The CNTs used in this work were refluxed in HNO_3 for 24 h and washed by rinsing and centrifugation with DI water for several times and dried in a vacuum oven. To synthesis CNT/graphene/MnO_2 hydrogel, a 2 mg mL^{-1} suspension of CNTs was prepared by the sonication of CNT (20 mg) in 10mL deionized water for approximately 6h. Then 8 mL DI water, 2 mL grapheme oxide (GO, 10 mg mL^{-1}) and 200 mg $KMnO_4$ crystallites were added into the above dispersion under sonication. The mixture containing CNT (1 mg mL^{-1}), GO (1 mg mL^{-1}) and $KMnO_4$ (10 mg mL^{-1}) was stirred at room temperature for 16 h. After that, the reaction mixture was washed with DI water for several times and centrifuged to collect precipitation. Next, 5 mL of DI water re-suspended precipitate (2mg mL^{-1}) was put into a glass bottle and thoroughly mixed with 500μL ascorbic acids solution (100 mg mL^{-1}) at 50ºC for 15 h to form a CNT/graphene/MnO_2 hydrogel (Scheme 1). The as-obtained samples were washed for several times with DI water, and then freeze-dried for 24 h to completely remove water. Finally, the CNT/graphene/MnO_2 aerogel was obtained and

labelled as CGMA (CNT/Graphene/MnO_2 Aerogel). In addition, frozen-dried CNTs/graphene/MnO_2 without ascorbic acid solution treatment, labelled as CGM in following section, were prepared as a comparison.

2.3 Characterization of synthesized CNTs/graphene/MnO_2 aerogel

The microscopic morphology of the samples was observed using a scanning electron microscope (SEM, JSM-6510LV, Japan) and a transmission electron microscope (TEM, JEM-2100, Japan). The surface properties of the samples were characterized by X-ray photoelectron spectroscopy (XPS, Thermo, USA). Nitrogen sorption measurement was performed with a Quantachrome NoVa 1200e. The specific surface area and the pore size distribution were calculated using the Braunauer-Emmett-Teller (BET) method.

To characterize the electrochemistry prosperities of the nanocomposite, 2.5 mg CNT/graphene/MnO_2 aerogel was dispersed in 500 μL ethanol and 5μL of such suspension (5 mg mL^{-1}) was casted onto the surface of the glassy carbon electrode (GCE, 3 mm in diameter, CH Instruments). Cyclic voltammetric and electrochemical impedance spectroscopy (EIS) measurements were carried out on a CHI 760e electrochemical workstation in a 0.5 M KCl solution containing 50 mM $K_3Fe(CN)_6$.

2.4 Fabrication of electrodes/paper sandwich device

As shown in Scheme 2, wax-printing draws hydrophobic and hydrophilic region on filter paper. The hydrophilic region of filter paper was designed for analyst loading and cell growth. Silver paste was used to draw conduct wire. Carbon paper (CP) was cut into desired size by paper cutter. Then one head of CP electrode (CPE) was attached to hydrophobic region of filter paper by silver paste leaving 2 mm length of the CPEs at the hydrophilic region of the filter paper. Thus, in all experiments, the size of working electrode is 1×2 mm^2, and counter electrode is 4×2 mm^2. Then, the wax-patterned filter paper was sandwiched between CPEs to assemble a two-electrode electrochemical device. Because filter paper can suck aqueous solutions to wet electrodes, only very low sample volume was required for testing. In following experiment, if not specified, 100μL PBS was loaded at hydrophilic region to conduct electrochemical measurement. To functionalize the CPE working electrode, 2 μL suspension containing CNT/graphene/MnO_2 aerogel in ethanol (5 mg mL^{-1}) was deposited on the CPE surface then 1μL Nafion that was diluted in ethanol (1:30, V/V) was casted. After drying for 15 min, the CPE/paper/CPE sandwich device was ready for use. By similar procedures, the CNT/graphene/MnO_2 (without ascorbic acid treatment) functionalized CPE was also fabricated as a control.

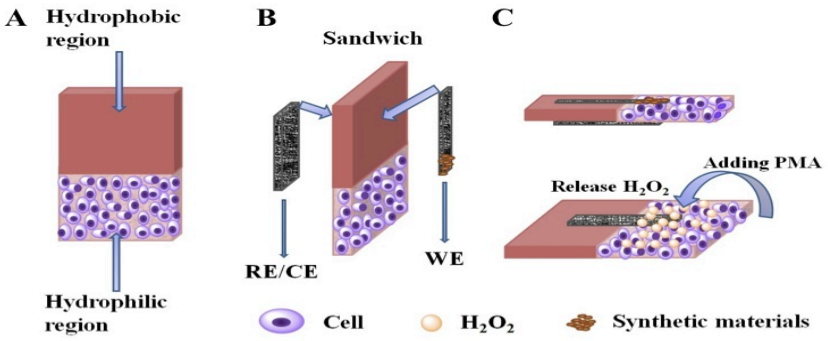

Scheme 2. Electrodes/paper sandwich device (A) wax-patterning of hydrophobic and hydrophilic region on filter paper (B) sandwich of carbon paper electrodes and wax-patterned paper. RE/CE: reference electrode/counter electrode; WE: working electrode (C) assembled electrodes/paper device and *in-situ* H_2O_2 detection. PMA: Phorbol 12-myristate-13-acetate

2.5 Electrochemical characterization of electrode/paper sandwich device

The setup of the CPE/paper/CPE sandwich device electrochemical measurement is shown in Scheme 2. Aperometric response of the device to H_2O_2 sensing was optimized through adjust the potential from -0.2 to -0.7 V. All potentials were measured and reported *vs.* the carbon paper counter electrode. The sensitivity of the CPE/paper sandwich device was monitored amperometrically at the working potential of −0.5 V *vs.* carbon paper counter electrode. In addition, the specificity of the CPE/paper sandwich device was demonstrated by measuring the amperometical response to dopamine (DA), uric acid (UA) and ascorbic acid (AA). All measurements were carried out in 0.1 M PBS (pH 7.0) and repeated at least three independent times.

2.6 *In situ* detection of extracellular H_2O_2 by electrode/cells-in-paper sandwich device

Human Larynx carcinoma cell HEp2 was maintained in RMPI containing 10% FBS plus 100 U mL^{-1} penicillin and 100 UmL^{-1} streptomycin. Cells were incubated in a humidified 37°C incubation chamber containing 5% CO_2. To facility the cell adhesion and growth on filter paper, cells were suspended in growth factor-free matrigel (BD Biosciences) at a final concentration of 4.5×10^6 cells mL^{-1}. The matrigelis a liquid at 4°C, and rapidly gels above 10°C. Unless specified otherwise, matrigel was diluted with ice cold cell suspension 1:5 (V/V). 40 μL of this ice-cold cell/matrigel suspension was spotted onto the pre-chilled filter paper using a pipette. Once the matrigel was solidified, the sandwiched two-electrode device was ready for *in situ* electrochemical measurement. Phorbol 12-myristate-13-acetate (PMA) was used as a model drug to trigger the production and release of hydrogen peroxide from cells. In brief, 2 μL PMA (100 μg mL^{-1}) was added on the filter paper embedding cell 3D growth to stimulate the release of H_2O_2. Then 4 μL catalase (5000 U mL^{-1}) was added to scavenge the produced H_2O_2. To further

prove the specificity of *in situ* H_2O_2 detection, an NADPH oxidase inhibitor diphenyleneiodonium (DPI) was used as a model reagent to block the PMA stimulated H_2O_2 production. To this aim, 0.4 μL DPI (10 mM L^{-1}) was incubated with 40 μL cell/matrigel suspensionfor 0.5 h. Then 2 μL PMA (100 μg mL^{-1}) was added. Amperometric responses were recorded by CHI-760e electrochemical station at applied potential of -0.5 *vs.* carbon paper counter electrode. All experiments were conducted in three independent times.

2.7 Statistical analysis

Results are expressed as means ± the standard deviation of the mean. The data were analyzed by Student's *t*-test using Origin Statistic software (Origin Lab Corporation, USA). A *p*-value < 0.05 was considered significant.

3. Results and discussion

3.1 Characterization of synthesized CNT/graphene/MnO_2 aerogel

Fig.1A shows SEM images of the CNT/graphene/MnO_2 aerogel with a typical wrinkled paper-like morphology of graphene. A high-magnified image of the same sample is presented as Fig.1A inset. Plentiful mesopores and macropores are found in the bulk of CNT/graphene/MnO_2 aerogel, suggesting the formation of a porous material. Surface area and pore-size distribution of the CNT/graphene/MnO_2 aerogel were quantified by nitrogen adsorption and desorption experiments. Nitrogen-adsorption and -desorption isotherms are shown in Fig1B. Using these isotherms, the multipoint Brunauer–Emmett–Teller (BET) specific surface areas the synthesized aerogel is 133.1 m^2g^{-1}. In addition, the pore-size distribution analysis shows a dominating sharp peak at 14nm and a broad peak, spanning from 30 to 85 nm, indicating that the aerogel is rich in hierarchical pores (Fig.1B inset).

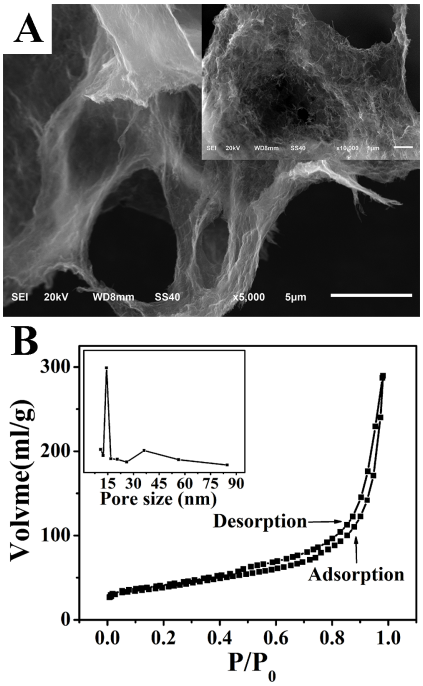

Fig.1 (A) SEM imaging of the synthetic materials CNT/graphene/MnO_2 aerogel (B) Nitrogen adsorption/desorption isotherm. Inset: pore-size distribution curve for N_2 of the aerogel

Fig.2A depicts corresponding TEM images of inherent structure of the CNT/graphene/MnO_2 aerogel, displaying a planar transparent sheet attached with nanotubes with the size of ~20-30 nm in width. In addition, well-distributed black dots can be observed on the graphene sheet and the size-wall of CNTs. Uniform dark dots with diameter of ~5 nm were ascertained from high-resolution TEM images. In addition, three lattice fringes with the spacing 0.21, 0.24 and 0.37 nm (B, C, D) were observed in one TEM photograph and can be indexed as (-112), (-111) and (002) crystal planes of α-type MnO_2 and graphene, respectively.[40]

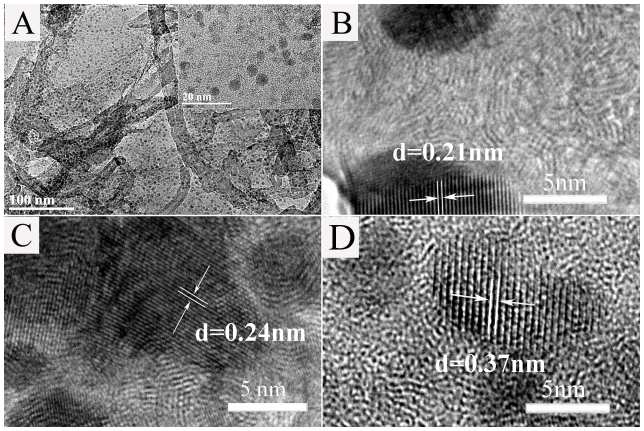

Fig. 2(A) TEM imaging of the synthetic materials CNT/graphene/MnO_2 aerogel; (B,C,D) the lattice of MnO_2 in CNT/graphene/MnO_2 aerogel.

Typical XPS spectra of the CNT/graphene/MnO_2 aerogel are shown in Fig.3A. Peaks of C 1s, O 1s and Mn (2p3/2, 2p1/2) can be observed from low to high binding energy. There are two peaks centered at 643.2 eV and 654.6 eV, with a spin-orbit splitting of 11.4 ev from zoomed in Mn2p3 peak (Fig.3B). According to previous report, peaks at 643.2 eV and 654.6 eV denote for Mn 2p3/2 and Mn 2p1/2.[31, 41] Based on the information derived from SEM, TEM and XPS characterizations, we conclude that through the reaction scheme as illustrated in Scheme 1, CNT/graphene/MnO_2 aerogel have been successfully synthesized. Next, we studied electrochemical properties of the CNT/graphene/MnO_2 aerogel by characterizing CNT/graphene /MnO_2 aerogel functionalized glass carbon electrode (GCE). As shown in Fig.4A, the highest Faradic current densities of $[Fe(CN)_6]^{3-}$ was observed from CNT/graphene/MnO_2 aerogel functionalized GCE (c), indicating the improved electrochemically active surface area by CNT/graphene aerogel structure and decorated nanometer size metallic nanocatalysts. Apparently, ascorbic acid treatment enables to form nanometer-sized MnO_2 decorated CNT/graphene aerogel with hierarchical pore size and surface area of 133.1 m^2 g^{-1} which may lead to an amplified real surface area of the electrode.[42] The EIS curve in Fig.4B further shows that CNT/graphene/MnO_2 aerogel functionalized GCE has a charge transfer resistance of 8 Ω (c), which is much smaller than those of CNT/graphene/MnO_2 (without ascorbic acid treatment)/GCE (82 Ω) and bare GCE electrode (110 Ω), confirming a faster electron transfer rate of CNT/graphene/MnO_2 aerogel nanocomposite to GCE.

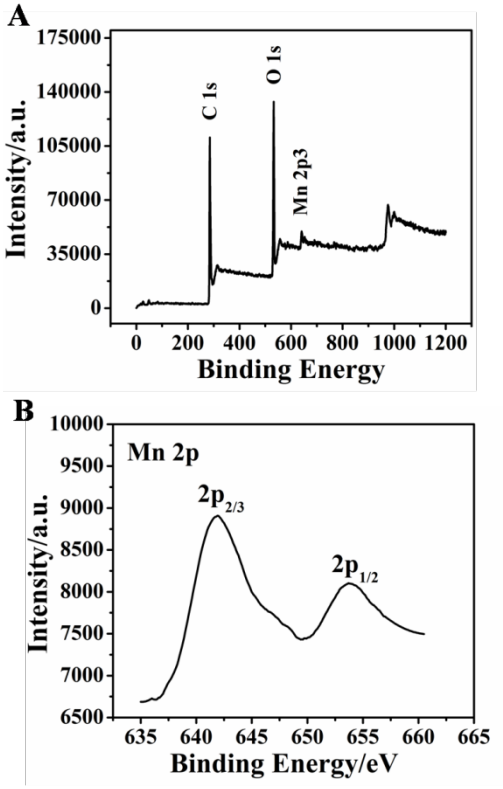

Fig.3 (A) XPS spectra of CNT/graphene/MnO_2 aerogel (B) Mn 2p XPS spectra of MnO_2.

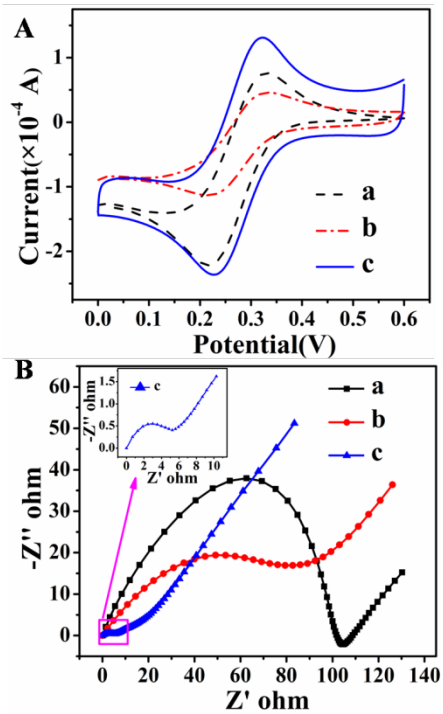

Fig.4 (A) CVs of bare glass carbon electrode (GCE) (a), CNT/graphene/MnO_2 (without ascorbic acid treatment) functionalized glass carbon electrode (CGM-GCE) (b) and CNT/graphene/MnO_2 aerogel functionalized glass carbon electrode (CGMA-GCE) (c) in 0.5 M KCl solution containing 50 mM $K_3Fe(CN)_6$ at the scan rate of 10 mVs^{-1}; (B) EIS of bare GCE (a), CGM-GCE (b) and CGMA-GCE electrode (c) in 0.5 M KCl solution containing 50 mM $K_3Fe(CN)_6$.

The above results suggest that the CNT/graphene/MnO_2 aerogel potentially gives rise to electrodes with enhanced catalytic activity. This may be related to the high surface area of graphene sheets along its planar structure providing large amount of anchoring sites for deposition of MnO_2 nanoparticles, while CNT assembled on graphene sheets improves electron transfer from graphene planar to electrode. The aerogel structure facilitates forming of hierarchical pores and preventing the aggregation of the nano-sized particles.

3.2 Electrode/paper sandwich device for hydrogen peroxide sensing

The response of fully assembled carbon paper electrode/paper sandwich devices (CPE/paper) to hydrogen peroxide was studied. Upon addition of 5 mM H_2O_2 to 0.1 M pH 7.0 PBS, the cyclic voltammogram (CV) of the CNT/graphene/MnO_2 aerogel functionalized electrode/paper device changed dramatically with an increase of reduction peak current (Fig.5A), while the CV changes of bare or CNT/graphene/MnO_2 (without ascorbic acid treatment) functionalized CPE and bare CPE were negligible (Fig.5B and C), displaying an obvious electro-catalytic behaviour of the CNT/graphene/MnO_2 aerogel to the reduction of H_2O_2. To demonstrate the specificity of cyclic vlotammgram response of fully assembled device to H_2O_2, catalase, a H_2O_2 scavenger[43] was added. As shown in Fig.5D, 2 mM H_2O_2 in 0.1 M pH7.0 PBS results in a reduction peak increase (b). The injection of catalase (c) leads to a return of CV curve back to PBS control (a).

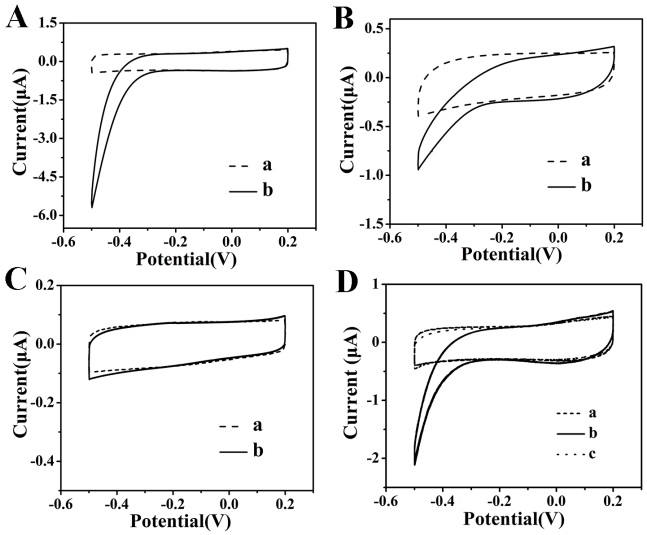

Fig.5 The voltammetric response of electrodes/paper sandwich device to H_2O_2 in PBS: (A) CNT/graphene/MnO_2 aerogel functionalized carbon paper electrode (B) CNT/graphene/MnO_2 (without ascorbic acid treatment) functionalized carbon paper electrode (C) bare carbon paper electrode; a: without H_2O_2 b: with 5 mM H_2O_2 (D) CNT/graphene/MnO_2 aerogel-carbon paper electrode, a: without H_2O_2, b with 2 mM H_2O_2, c: added catalase into 2 mM H_2O_2

To achieve real-time sensing H_2O_2 production, attention has been paid on amprometric detection of hydrogen peroxide. To record the amperometric signals, the choice of the applied potential at the working electrode is critical to achieve the lowest detection limit and to avoid electrochemical interfering species. As shown in Fig.6A, the net steady state redox responses of 0.2 mM H_2O_2 on CNT/graphene/MnO_2 aerogel (CGMA) functionalized carbon

paper electrode (CGMA-CPE) under potentials between -0.2 V and −0.7 V were recorded. The background current of CGMA-CFP was low over the potential range tested (-0.2 V to −0.4 V) (Fig.6A, black line). A rapid increase in the magnitude of background current started at −0.5 V. In comparison, the net reductive currents of CGMA-CPE to 0.2 mM H_2O_2 at potentials of −0.4 V, −0.5 V, −0.6 V and -0.7 V are 0.4 μA, 0.8 μA, 1.2 μA and 1.7 μA, respectively (Fig.6A, red line). To achieve a sensitive response while effectively avoid interference, -0.5 V was selected as the applied potential in subsequent experiments.

Ascorbic acid (AA), dopamine (DA) and uric acid (UA) are potential interferences co-existing with hydrogen peroxide in biological samples.[44] To demonstrate the selectivity of the CNT/graphene/MnO_2 aerogel functionalized sandwich device against H_2O_2, amperometric response of the device to individually analyse H_2O_2 and common interferences were measured. The current response to AA, DA and UA is significant lower than that to H_2O_2 indicating that fully assembled sandwich device could specific response to H_2O_2. The interference concentration tested in this study is 0.2 mM which is at the maximum range of physiological concentration of AA, DA and UA.[45-47] Herein, the results demonstrate that CNT/graphene/MnO_2 aerogel equipped device capable for selectively testing H_2O_2 in a biological sample (Fig.6B).

Fig.6C shows typical amperometric response of the CNT/graphene/MnO_2 aerogel functionalized sandwich device to subsequent addition of H_2O_2 in PBS at -0.5 V. It is observed that the fully assembled sandwich device responds quickly to the change of H_2O_2 concentration. A trend of current drop can be observed during the extended measurement. This may be caused by the decease of H_2O_2 concentration in the vicinity area. The current-dose response curve calculated from three independent measurements is shown in inset of Fig. 6C. The device displays a broad linear range up to 25 mM, much superior to various H_2O_2 sensing platform (Table1). The sensitivity of the fully assembled devices is 6.25 $\mu A mM^{-1} cm^{-2}$, based on the ratio of the slope of current-dose response curve and the surface area of electrode.[25] In addition, the device achieves a low detection limit of 6.7 μM based on noise to ratio of 3 (Fig.6D). Comparing to existing platforms shown in Table1, the fully assembled electrode/paper sandwich device demonstrates its potential as a disposable device for H_2O_2 sensing with a broad working range. The electrodes/paper sandwich structure can assay as low as 40 μL sample, significantly reducing the sample volume for sensing. This is important for rare biological samples, such as clinical biopsy, analysis.

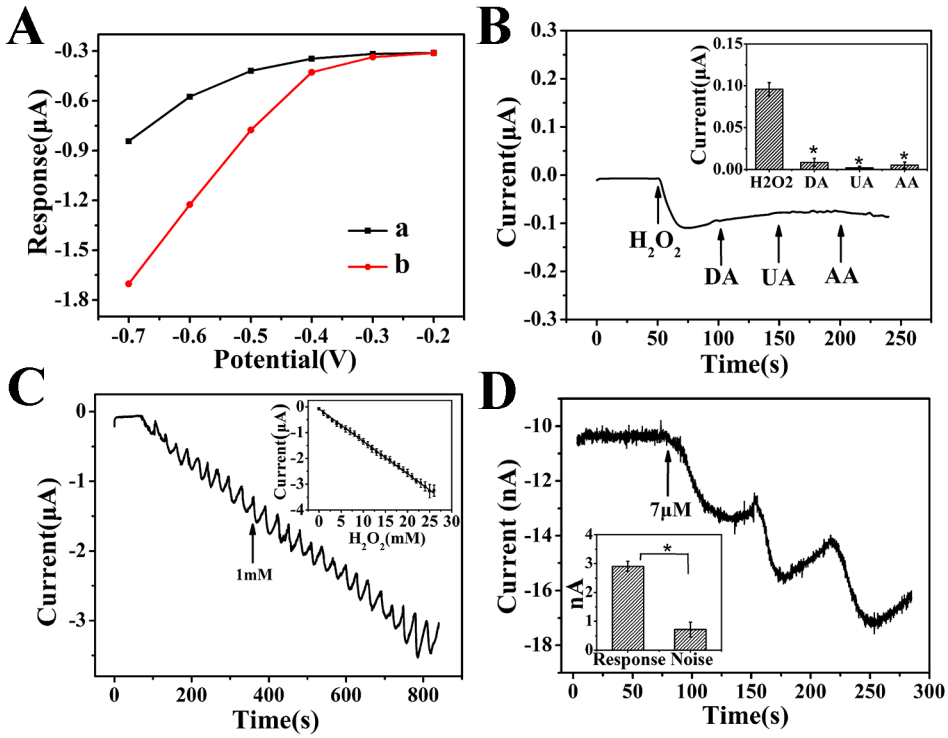

Fig.6 Characterization of fully assembled CNT/graphene/MnO_2 aerogel functionalized carbon paper electrode (CGMA-CPE)/paper sandwich electrochemical device: (A) The optimal working potential for electrode/paper sandwich device was studied by using H_2O_2 as a model. Constant reductive currents were measured in PBS (pH 7.0) without (black) or with 0.2 mM H_2O_2 (red) under potentials ranging from -0.2 to −0.7 V. (B) Effect of interfering species on the biosensor response: H_2O_2 (1.0 mM), dopamine (DA, 0.2 mM), uric acid (UA, 0.2 mM), ascorbic acid (AA, 0.2 mM). The histogram was calculated from three independent tests (* denotes $p< 0.05$) (C) Amperometric response of CGMA-CPE/paper sandwich device to successive additions of 1 mM of H_2O_2 was determined in PBS at an applied potential of -0.5 V; the inset is calibration curve between the current response and concentration of H_2O_2 (n=3). (D) Typical current change in response of CGMA-CPE/paper sandwich device to low concentration of H_2O_2 in PBS; the inset is histogram of noise signal and current change in response of 7 μM H_2O_2 (n=3, * denotes $p< 0.05$)

Cite this: DOI: 10.1039/c0xx00000x

www.rsc.org/xxxxxx

ARTICLE TYPE

Table 1 Comparison of various H2O2 sensing platforms

Sensing Material	*H2O2 detection performance*			*platform*			*Living cell detection*	*Ref*
	linear range μM	Sensitivity $\mu A \mu M^{-1} cm^{-2}$	Detection limit μM	Electrode	Fully assembled device	disposable		
CNT/Graphene/MnO_2	7-25000	0.00625	6.7	Carbon paper	YES	YES	YES	a
Layered graphene/PB	0.1-100	4.50	0.10	ITO	NO	YES	YES	25
PB/Carbon nanotubes	5-2200	0.86	5.0	ITO	NO	YES	NO	26
PB/Mesoporous carbons	-	0.28	1.0	GCE	NO	NO	NO	27
Cytochrome *c*/ TiO_2nanoneedles	0.85-24 000	-	0.26	ITO	NO	YES	YES	48
HRP–HAP	5-820	-	0.1	GCE	NO	NO	YES	36
MnO_2/DHP	12–2000	0.266	0.08	GCE	NO	NO	NO	49
MnO2	12-260	0.00075	5.4	Carbon fiber	NO	YES	NO	50
PPy-HRP	100-2000	0.03324	-	SPE	YES	YES	NO	51
HRP-Au	0.8-1000	0.3067	0.4	SPE	YES	YES	NO	52
Bulk PB	0.4–100	0.137	0.4	SPE	YES	YES	NO	53
Oxygen plasma treated carbon	200-2000	-	-	thick-film carbon	YES	YES	NO	54

a : this work; PB: prussion blue; HRP: horseradish peroxidase; HAP: hydroxyapatite nanohybrids; DHP: dihexadecyl hydrogen phosphate; PPy: Polypyrrole; Au: gold; Indium tin oxide: ITO; GCE: glass carbon electrode; SPE: screen printed electrode

3.3 CNT/graphene/MnO_2 nanocompoiste functionalized sandwich device *in situ* monitoring of H_2O_2 secretion from living cells

For *in situ* electrochemical sensing of H_2O_2 secretion, human larynx carcinoma HEp2 cells were directly grown on the matrigel impregnated paper that was sandwiched between carbon paper electrodes. The *in situ* monitoring of H_2O_2 released was investigated by using a model drug phorbol 12-myristate-13-acetate (PMA), a chemical known to trigger hydrogen peroxide production from human cells.[55] The amperometric response at the applied potential of -0.5 V was recorded when PMA was added on gels-in-paper containing ~2×10^5 cell. In addition, a NADH-ubiquinone oxidoreductase inhibitor diphenyleneiodonium (DPI) [56] and a H_2O_2 scavenger, catalase,[43] were measured along with PMA to investigate the specificity of *in situ* monitoring of H_2O_2 secreted from cells. As presented in Fig.7A, injection of PMA (5 μg mL^{-1}) can sharply increase reduction peak current (line: cell response 4), while no current response was observed from device without cell (line: control) and device with cultured cells under vector (dimethyl sulfoxide, DMSO) injection (line: cell response1). PMA induced current change is significantly diminished by DPI that is known to inhibit the production of H_2O_2 by mitochondrial respiration (line: cell response 2). Moreover, with the addition of catalase that can decompose hydrogen peroxide to water and oxygen, the reduction peak current increased caused by PMA injection decreases sharply (line: cell response 3).

Fig.7B shows the histogram of current changes based on 3 independent tests. 4 μL PMA (5 μg mL^{-1}) can stimulate cells secret H_2O_2 which is characterized by a 9.94 nA current change. The number of extracellular H_2O_2 molecule released per cell (No) can be calculated according to a formula reported by Guo *et al*[25]:

$$No = \{\Delta R \div (k \times A) \times V\} \times N_A \div Nc$$

where ΔR is current response, *k* is sensitivity of the sensing platform, A is electrode surface area, V is volume of electrolyte, N_A is the Avogadro constant (6.02×10^{23}/mole), and Nc is cell number. With known response of 9.94 nA, a sensitivity of 6.25 μA mM^{-1} cm^{-2}, sensing electrode area of 2 mm^2, and ~2×10^5 cells, as well as the volume of the electrolyte (40 μL), No can be calculated, around 1.06×10^{11} which is well in-line with literature reported data.[25]

More importantly, the current response clearly shows that incubation with DPI can decrease the PMA induced current change to 2 nA, demonstrating the capability of real time monitoring drug effect. Collectively, the results confirm that the amperometric responses are directly generated from H_2O_2 secreted by larynx carcinoma HEp2 cells, demonstrating the *in situ* sensing of small molecular released by cells growing in gels-in-paper matrix. The freestanding electrodes/paper sandwich device can be a potent candidate for real-time monitoring live secretion of electroactive substances from cells growing in microenvironment mimic *in vivo* conditions.

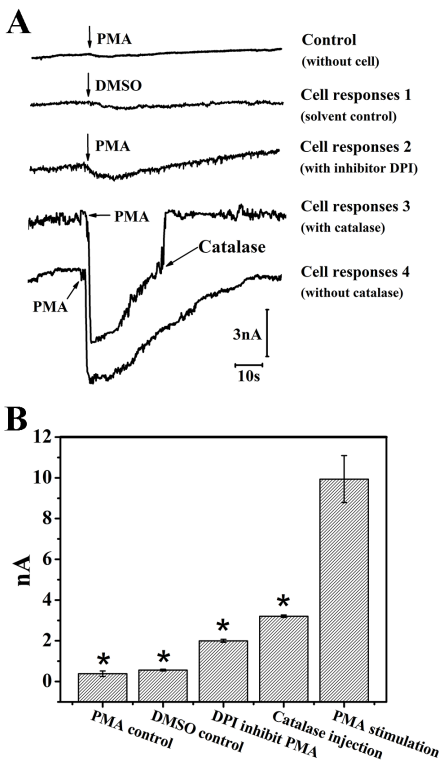

Fig.7(A) Amperometric responses of CNT/graphene/MnO_2 aerogel functionalized carbon paper electrode (CGMA-CPE) /paper sandwich device without cells under PMA injection (control: without cell), CGMA-CPE/paper sandwich device with cultured cells under injection of DMSO (cell response 1: solvent control), CGMA-CPE/paper sandwich device with cells and DPI under PMA injection (cell response 2: with DPI inhibitor), CGMA-CPE/paper sandwich device with cultured cells under PMA injection, followed by catalase injection (cell response 3: with catalase) and CGMA-CPE/paper sandwich device with cultured cells under PMA injection (cell response 4: without catalase). (B) the corresponding current response obtained from amperometric curves of three independent experiments, (n=3, * denotes $p<0.05$). PMA: phorbol 12-myristate-13-acetate, DPI: diphenyleneiodonium

4. Conclusion

In summary, we have demonstrated a new type of freestanding electrode/paper sandwich device by arranging one-layer of paper between face-to-face arranged working electrode and counter electrode. Because, the filter paper in the device can suck aqueous sample to wet electrodes for electrochemical measurement, small sample volume was required for assay. CNT/graphene/MnO_2 aerogel nanocomposite has been synthesized to functionalize carbon paper electrode. The fully assembled electrode/paper sandwich devices were employed for determination of hydrogen peroxide. The freestanding device displays a linear range up to 25 mM with a sensitivity of 6.25 μA $mM^{-1}cm^{-2}$, and a detection limit of 6.7 μM H_2O_2 in PBS. Due to the intimate contact of the sandwiched paper with electrodes, H_2O_2 released from cells growing in paper matrix was monitored real-timely. We envision that our modular approach for designing flexible electrodes/paper sandwich devices with functional material decorating would offer new insights on designing low-cost disposable miniaturized biosensors for cell biology investigations.

Acknowledgements

This work is financially supported by the National Program on Key Basic Research Project of China (973 Program) under contractNo.2013CB127804, National Science Foundation of China (No. 31200700，21375108), Fundamental Research Funds for the Central Universities (XDJK20132013C059), Institute for Clean Energy & Advanced Materials (Southwest University, Chongqing, China), Chongqing Key Laboratory for Advanced Materials and Technologies of Clean Energies (Chongqing, China), Start-up grant under SWU111071 from Southwest University (Chongqing, China)， Chongqing Engineering Research Center for Rapid diagnosis of Dread Disease (Chongqing, China) and Chongqing development and reform commission (Chongqing, China).

Notes and references

a. Institute for Clean Energy & Advanced Materials, Southwest University, Chongqing 400715, China
b. Chongqing Key Laboratory for Advanced Materials and Technologies of Clean Energies, Chongqing 400715, China
c. Faculty of Materials and Energy, Southwest University, Chongqing, 400715, China
**Corresponding authors: Tel: +86-23-68254842; E-mail: lingyu12@swu.edu.cn*

1. P. Lisowski and P. K. Zarzycki, *Chromatographia*, 2013, **76**, 1201-1214.
2. A. Nilghaz, D. H. B. Wicaksono, D. Gustiono, F. A. A. Majid, E. Supriyanto and M. R. A. Kadir, *Lab Chip*, 2012, **12**, 209-218.
3. A. K. Ellerbee, S. T. Phillips, A. C. Siegel, K. A. Mirica, A. W. Martinez, P. Striehl, N. Jain, M. Prentiss and G. M. Whitesides, *Analytical chemistry*, 2009, **81**, 8447-8452.
4. A. W. Martinez, S. T. Phillips, M. J. Butte and G. M. Whitesides, *Angew Chem Int Ed Engl*, 2007, **46**, 1318-1320.
5. A. W. Martinez, S. T. Phillips, G. M. Whitesides and E. Carrilho, *Analytical chemistry*, 2010, **82**, 3-10.
6. Z. Nie, F. Deiss, X. Liu, O. Akbulut and G. M. Whitesides, *Lab Chip*, 2010, **10**, 3163-3169.
7. S. N. Tan, L. Ge, H. Y. Tan, W. K. Loke, J. Gao and W. Wang, *Analytical chemistry*, 2012, **84**, 10071-10076.
8. P. Wang, L. Ge, M. Yan, X. Song, S. Ge and J. Yu, *Biosensors & bioelectronics*, 2012, **32**, 238-243.
9. W. Liu, C. L. Cassano, X. Xu and Z. H. Fan, *Analytical chemistry*, 2013, **85**, 10270-10276.
10. B. Li, W. Zhang, L. Chen and B. Lin, *Electrophoresis*, 2013, **34**, 2162-2168.
11. D. Zang, L. Ge, M. Yan, X. Song and J. Yu, *Chem Commun (Camb)*, 2012, **48**, 4683-4685.
12. K. Ziolkowska, R. Kwapiszewski and Z. Brzozka, *New J Chem*, 2011, **35**, 979-990.
13. C. P. Huang, J. Lu, H. Seon, A. P. Lee, L. A. Flanagan, H. Y. Kim, A. J. Putnam and N. L. Jeon, *Lab Chip*, 2009, **9**, 1740-1748.
14. L. Yu, S. R. Ng, Y. Xu, H. Dong, Y. J. Wang and C. M. Li, *Lab Chip*, 2013, **13**, 3163-3182.
15. R. Derda, S. K. Tang, A. Laromaine, B. Mosadegh, E. Hong, M. Mwangi, A. Mammoto, D. E. Ingber and G. M. Whitesides, *PLoS One*, 2011, **6**, e18940.

16. F. Deiss, A. Mazzeo, E. Hong, D. E. Ingber, R. Derda and G. M. Whitesides, *Analytical chemistry*, 2013, **85**, 8085-8094.
17. R. Derda, A. Laromaine, A. Mammoto, S. K. Tang, T. Mammoto, D. E. Ingber and G. M. Whitesides, *Proc Natl Acad Sci U S A*, 2009, **106**, 18457-18462.
18. H. Cai, *Cardiovascular research*, 2005, **68**, 26-36.
19. M. L. Circu and T. Y. Aw, *Free Radic Biol Med*, 2010, **48**, 749-762.
20. S. Varma and C. K. Mitra, *Electrochem Commun*, 2002, **4**, 151-157.
21. Z. Matharu, J. Enomoto and A. Revzin, *Analytical chemistry*, 2013, **85**, 932-939.
22. Y. Zou, L. X. Sun and F. Xu, *Biosensors & bioelectronics*, 2007, **22**, 2669-2674.
23. Z. Chu, L. Shi, Y. Liu, W. Jin and N. Xu, *Biosensors & bioelectronics*, 2013, **47**, 329-334.
24. P. H. Lo, S. A. Kumar and S. M. Chen, *Colloids Surf B Biointerfaces*, 2008, **66**, 266-273.
25. C. X. Guo, X. T. Zheng, Z. S. Lu, X. W. Lou and C. M. Li, *Adv Mater*, 2010, **22**, 5164-5167.
26. J. Zhai, Y. Zhai, D. Wen and S. Dong, *Electroanal*, 2009, **21**, 2207-2212.
27. J. Bai, B. Qi, J. C. Ndamanisha and L. P. Guo, *Micropor Mesopor Mat*, 2009, **119**, 193-199.
28. Y. H. Lin, X. L. Cui and L. Y. Li, *Electrochem Commun*, 2005, **7**, 166-172.
29. L. Zhang, Z. Fang, Y. H. Ni and G. C. Zhao, *Int J Electrochem Sc*, 2009, **4**, 407-413.
30. L. M. Li, Z. F. Du, S. A. Liu, Q. Y. Hao, Y. G. Wang, Q. H. Li and T. H. Wang, *Talanta*, 2010, **82**, 1637-1641.
31. D. X. Ye, H. X. Li, G. H. Liang, J. Luo, X. X. Zhang, S. Zhang, H. Chen and J. L. Kong, *Electrochim Acta*, 2013, **109**, 195-200.
32. Y. Chen, Y. Zhang, D. S. Geng, R. Y. Li, H. L. Hong, J. Z. Chen and X. L. Sun, *Carbon*, 2011, **49**, 4434-4442.
33. Y. Wang, Z. H. Li, J. Wang, J. H. Li and Y. H. Lin, *Trends Biotechnol*, 2011, **29**, 205-212.
34. M. Liu, R. Liu and W. Chen, *Biosensors & bioelectronics*, 2013, **45**, 206-212.
35. D. Chen, L. Tang and J. Li, *Chemical Society reviews*, 2010, **39**, 3157-3180.
36. C. Li, H. Zhang, P. Wu, Z. Gong, G. Xu and C. Cai, *The Analyst*, 2011, **136**, 1116-1123.
37. S. Yao, J. Xu, Y. Wang, X. Chen, Y. Xu and S. Hu, *Analytical Chimica Acta*, 2006, **557**, 78-84.
38. J. F. Zhai, Y. M. Zhai, D. Wen and S. J. Dong, *Electroanal*, 2009, **21**, 2207-2212.
39. J. T. Zhang, Z. G. Xiong and X. S. Zhao, *J Mater Chem*, 2011, **21**, 3634-3640.
40. H. G. Wang, Z. G. Lu, D. Qian, Y. J. Li and W. Zhang, *Nanotechnology*, 2007, **18**, 115616.
41. J. Yan, Z. J. Fan, T. Wei, W. Z. Qian, M. L. Zhang and F. Wei, *Carbon*, 2010, **48**, 3825-3833.
42. X. Zan, Z. Fang, J. Wu, F. Xiao, F. Huo and H. Duan, *Biosensors & bioelectronics*, 2013, **49**, 71-78.
43. H. N. Kirkman and G. F. Gaetani, *Proc Natl Acad Sci U S A*, 1984, **81**, 4343-4347.
44. C. Wang, R. Yuan, Y. Chai, S. Chen, F. Hu and M. Zhang, *Analytica chimica acta*, 2012, **741**, 15-20.
45. J. W. Mo and B. Ogorevc, *Analytical chemistry*, 2001, **73**, 1196-1202.
46. E. P. de Oliveira and R. C. Burini, *Diabetology & metabolic syndrome*, 2012, **4**, 12.
47. G. Capasso, P. Jaeger, W. G. Robertson and R. J. Unwin, *Current pharmaceutical design*, 2005, **11**, 4153-4159.
48. Y. Luo, H. Liu, Q. Rui and Y. Tian, *Analytical chemistry*, 2009, **81**, 3035-3041.
49. S. Yao, J. Xu, Y. Wang, X. Chen, Y. Xu and S. Hu, *Analytica chimica acta*, 2006, **557**, 78-84.
50. S. B. Hocevar, B. Ogorevc, K. Schachl and K. Kalcher, *Electroanalysis*, 2004, **16**, 1711-1716.
51. G. Li, Y. Wang and H. Xu, *Sensors*, 2007, **7**, 239-250.
52. X. Xu, S. Liu and H. Ju, *Sensors*, 2003, **3**, 350-360.
53. M. P. O'Halloran, M. Pravda and G. G. Guilbault, *Talanta*, 2001, **55**, 605-611.
54. E. J. Kim, T. Haruyama, Y. Yanagida, E. Kobatake and M. Aizawa, *Analytica chimica acta*, 1999, **394**, 225-231.
55. S. Chakraborti and T. Chakraborti, *Cellular signalling*, 1995, **7**, 75-83.
56. D. R. Gallie, H. Le, C. Caldwell and K. S. Browning, *Biochemical and biophysical research communications*, 1998, **245**, 295-300.